Applied Catalysis A: General 388 (2010) 179–187

Contents lists available at ScienceDirect

Applied Catalysis A: General

journal homepage: www.elsevier.com/locate/apcata

Larock indole synthesis using palladium complexes immobilized onto mesoporous silica

Nelly Batail [a], Anissa Bendjeriou [b], Laurent Djakovitch [a,**], Véronique Dufaud [b,*]

[a] Université de Lyon, CNRS, UMR 5256, IRCELYON, Institut de recherches sur la catalyse et l'environnement de Lyon, 2 avenue Albert Einstein, F-69626 Villeurbanne, France
[b] Université de Lyon, CNRS, UMR 5182, Laboratoire de Chimie, Ecole Normale Supérieure de Lyon, 46 Allée d'Italie, F-69364 Lyon Cedex 07, France

ARTICLE INFO

Article history:
Received 22 June 2010
Received in revised form 20 August 2010
Accepted 23 August 2010
Available online 23 September 2010

Keywords:
Indoles
SBA-15
Palladium catalysts
Larock synthesis
Heterogenous catalysis

ABSTRACT

Heterogeneous palladium catalysts were prepared by covalent immobilization of palladium (II) complexes of the general formula $PdCl_2L_2$ (L = P, CN) onto SBA-15 silica using a post-synthetic method. The state of the hybrid materials was characterized using a wide variety of molecular and solid-state techniques. In general, all the palladium modified solids exhibited highly ordered mesostructures while keeping the integrity of the parent molecular precursors. The catalytic performances of the materials were evaluated in the heteroannulation of 2-iodoaniline and 2-bromoaniline with triethyl(phenylethynyl)silane which showed high activities and selectivities with isolated yields in the range of 80–85%. Despite a decrease in the initial activity, quantitative conversion of iodoaniline to the expected product was observed over multiple recyclings, making these materials particularly efficient for such applications. The catalytic process was shown to be homogeneous in nature, the solid apparently serving as a "reservoir" for the metal between cycles.

1. Introduction

The indole nucleus is an important substructure found in numerous natural or synthetic alkaloids [1,2]. The diversity of the structures encountered, as well as their biological and pharmaceutical relevance, have motivated research aimed at the development of new economical, efficient and selective synthetic strategies, particularly for the synthesis of functional indole rings [3–6]. Classical methods include the Fischer indole synthesis from aryl hydrazone, the Batcho–Leimgruber synthesis from *o*-nitrotoluenes and dimethylformamide acetals, the Gassman synthesis from *N*-haloanilines, the Madelung cyclization of *N*-acyl-*o*-toluidines and the reductive cyclization of *o*-nitrobenzyl ketones. While these procedures have contributed to this important area, the synthesis of functional indoles has proven challenging.

Recently, transition-metal catalyzed transformations, and particularly palladium catalyzed reactions, have been developed, providing increased tolerance toward functional groups and generally leading to higher reaction yields [7–16]. Many of these methods have proven to be most powerful and are currently applied in the target- or the diversity-oriented synthesis of multi-functional indoles. Recently, the palladium catalyzed heteroannulation of 2-iodoanilines with internal alkynes known as the Larock indole synthesis (Fig. 1) has emerged as one of the most powerful synthetic procedure to provide access to 2,3-substituted indoles [17–22].

However, these Larock procedures rely on the use of soluble palladium catalysts (featuring often costly phosphine ligands), leading to significant difficulties including the separation of the catalytic material from the reaction mixture, lack of adequate catalyst recycling methods and relatively high palladium and ligand contamination of the products. The latter problems are intolerable in the context of biological applications. Obviously, an analogous catalytic heterogeneous method would eliminate any of these drawbacks [23–26].

With the aim of resolving this issue we reported previously the first successful use of heterogeneous palladium catalysts (Pd/C, [Pd]/NaY) at low loadings (2 mol%) for indole syntheses under ligand- and salt-free reaction conditions [27]. While the resulting protocol featured reasonably priced reagents and solvents rendering the method competitive, practicable, and scalable it remained limited due to relative lack of catalysts activity and recyclability.

In order to propose advanced protocols featuring highly active and recyclable catalysts we undertook the development of hybrid materials based on the SBA-15 mesoporous silica modified by grafted palladium complexes bearing either phosphine or cyano ligands. In this contribution, we describe the preparation and the characterization of these new catalysts and their successful application to the "salt-free" Larock indole syntheses. To fulfil economical considerations, we used exclusively technical grade solvent for the catalytic runs and demonstrated that the procedure tolerates very

* Corresponding author. Tel.: +33 472728857; fax: +33 472728860.
** Corresponding author. Tel.: +33 472445381; fax: +33 472445399.
E-mail addresses: Laurent.Djakovitch@ircelyon.univ-lyon1.fr (L. Djakovitch), vdufaud@ens-lyon.fr (V. Dufaud).

0926-860X/$ – see front matter © 2010 Elsevier B.V. All rights reserved.
doi:10.1016/j.apcata.2010.08.046

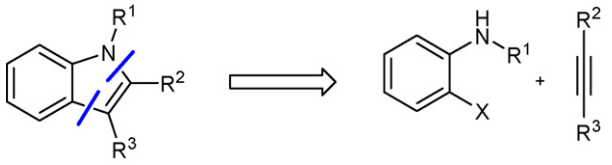

Fig. 1. Retro-synthetic approach toward the synthesis of indole nucleus following the Larock palladium catalyzed methodology.

low catalyst loading (1 mol%) compared to those reported generally for such syntheses under homogeneous conditions. Furthermore, we evidenced the high recyclability of the catalytic materials.

2. Experimental section

All manipulations were conducted under a strict inert atmosphere or vacuum conditions using Schlenk techniques including the transfer of the catalysts to the reaction vessel. In the case of catalysts synthesis, the solvents were dried using standard methods and stored over activated 4 Å molecular sieves. Tetraethoxysilane (TEOS) and poly(ethyleneoxide)-poly(propyleneoxide)-poly (ethyleneoxide) block copolymer (Pluronic 123, Mw: 5000) were purchased from Aldrich Chemical and used without further purification. Palladium chloride, diphenylphosphine and dicyclohexylphosphine were obtained from Fluka. 2-(diphenylphosphino) ethyltriethoxysilane, 3-cyanopropyltriethoxysilane, 3-aminopropyltriethoxysilane and 3-chloropropyltriethoxysilane were purchased from ABCR and stored under nitrogen. 3-(dicyclohexylphosphino)propyltriethoxysilane was cleanly obtained through a one pot two-step synthesis by first reacting dicyclohexylphosphine with *n*-BuLi at 0 °C followed by addition to the reaction mixture of 3-chloropropyltriethoxysilane at −78 °C. After stirring at room temperature another 20 h the desired product was purified by distillation under reduced pressure (73% yield, b.p. 150 °C (15 mm)) [35]. 3-{bis[(diphenylphosphanyl)methyl]amino} propyltriethoxysilane was prepared in high yield by reacting 3-aminopropyltriethoxysilane with paraformaldehyde and diphenylphosphine in refluxing toluene as described by Del Zotto et al. [36]. Both bifunctional phosphines were characterized by ^{31}P, ^{1}H and ^{13}C NMR spectroscopy and the results are in good accord with those reported in the literature. $PdCl_2(PhCN)_2$ and (3-cyanopropyltriethoxysilane) palladium dichloride, $PdCl_2(NC(CH_2)_3Si(OEt)_3)_2$ 4, were prepared according procedures previously described in the literature from $PdCl_2$ and respectively benzonitrile and 3-cyanopropyltriethoxysilane at 80 °C during 2 days [37,38].

Low-angle X-ray powder diffraction (XRD) data were acquired on a Bruker D5005 diffractometer using Cu Kα monochromatic radiation (λ = 1.054184 Å). Nitrogen adsorption–desorption isotherms at 77 K were measured using a Micromeritics ASAP 2010M physisorption analyzer. The samples were evacuated at 160 °C for 24 h before the measurements. Specific surface areas were calculated following the BET procedure. Pore size distribution was obtained using the BJH pore analysis applied to the desorption branch of the nitrogen adsorption/desorption isotherm. Infrared spectra were recorded from KBr pellets using a Mattson 3000 IRFT spectrometer. A Netzsch thermoanalyser STA 409PC was used for simultaneous thermal analysis combining thermogravimetric (TGA) and differential thermoanalysis (DTA) at a heating rate of 10 °C min^{-1} in air from 25 to 1000 °C. Solid-state NMR MAS and CP-MAS experiments were performed on a Bruker DSX 400 spectrometer at spectral frequencies of 161.99, 79.49 and 100.63 MHz for respectively ^{31}P, ^{29}Si and ^{13}C nuclei. Chemical shifts were referenced to 85% aqueous H_3PO_4 for ^{31}P NMR and to TMS for ^{29}Si and ^{13}C. A 4 mm triple resonance Bruker MAS probe was used for CP-MAS on ^{29}Si and ^{13}C. The spinning rate for both was 10 kHz and samples were spun at the magic angle using ZrO_2 rotors. The experimental details for the ^{29}Si and ^{13}C CP-MAS NMR experiments were as follows: contact time: 5 and 3 ms respectively, 90° ^{1}H transmitter pulse length: 3 μs, number of scans: 15,000–50,000 and repetition time: 4 s. ^{31}P CP-MAS experiments were performed with a 2.5 mm double resonance Brucker MAS probe at a spinning rate of 20 kHz. Contact time was set to 2 ms, repetition time to 10 ms and the number of scans was fixed at 20,000 with a 90° ^{1}H transmitter pulse of 2.85 μs. High-resolution electron microscopy was carried out with a JEM 2010 (Cs = 0.5 mm) microscope. The accelerating voltage was 200 kV with LaB_6 emission current, a point resolution of 0.19 nm, and a useful limit of EDS LINK-ISIS. Energy-dispersive X-ray microanalysis (EDX) was conducted using a probe size of 25–100 nm to analyze grains of the phases. Samples were sonically dispersed in ethanol and deposited on a holey carbon copper grid before examination. XPS measurements were recorded on a Kratos Axis Ultra DLD spectrometer, using a monochromated Al Kα X-ray source with a pass energy of 20 eV. The measurements of the binding energies were referred to the characteristic C 1s peak of the carbon fixed at the generally accepted value of 285.0 eV. Metal determinations were performed by ICP-AES (Activa Jobin Yvon) spectroscopy from a solution obtained by treatment of the solid catalyst with a mixture of HF, HNO_3 and H_2SO_4 in a Teflon reactor at 150 °C. Liquid NMR spectra were recorded on a BRUKER AC-250 spectrometer. All chemical shifts were measured relative to residual ^{1}H or ^{13}C NMR resonances in the deuterated solvents: $CDCl_3$, δ 7.26 ppm for ^{1}H, 77.0 ppm for ^{13}C; DMSO, δ 2.50 ppm for ^{1}H, 39.5 ppm for ^{13}C. Data are reported as follows: chemical shift, multiplicity (s = singlet, d = doublet, t = triplet, q = quartet, m = multiplet, br = broad). Melting points were determined in open capillary tubes and are uncorrected. Analytical thin layer chromatography (TLC) was performed on Fluka Silica Gel 60 F_{254}. GC analyses were performed on a HP 4890 chromatograph equipped with a FID detector, a HP 6890 autosampler and a HP-5 column (cross-linked 5% phenyl-methylsiloxane, 30 m × 0.25 mm i.d. × 0.25 μm film thickness) with nitrogen as carrier gas. GC–MS analyses were obtained on a Shimadzu GC-MS-QP2010S equipped with a Sulpelco SLB-5MS column (95% methylpolysiloxane + 5% phenylpolysiloxane, 30 m × 0.25 mm × 0.25 μm) with Helium as carrier gas. Conversions were determined by GC based on the relative area of GC-signals referred to an internal standard (biphenyl) calibrated to the corresponding pure compounds. The experimental error was estimated to be Δrel = ±5%. Chemical yields refer to pure isolated substances. Purification of products was accomplished by flash chromatography performed at a pressure slightly greater than atmospheric pressure using silica (Macherey-Nagel Silica Gel 60, 230–400 mesh) with the indicated solvent system.

2.1. Synthesis of homogeneous organophosphine palladium catalysts

A series of phosphine-based palladium complexes of the type, $PdCl_2L_2$, with L = mono- or diphosphine, was synthesized by reacting the appropriate amount of phosphine ligand (1 or 2 equivalents respectively for di- and monophosphine) with bis(benzonitrile)palladium dichloride at room temperature in methylene chloride by adapting a procedure reported elsewhere [35].

2.1.1. Bis {(diphenylphosphino)propyltriethoxysilane)palladium dichloride, 1

Yield: 95% as a yellow solid; ^{31}P {^{1}H} NMR (81 MHz, $CDCl_3$, 25 °C) δ 21.4 (s, *trans* isomer), 31.7 (s, *cis* isomer); ^{13}C NMR

(50 MHz, $CDCl_3$, 25 °C) δ 4.1 (s, CH_2Si), 18 (s, CH_3CH_2O), 18.9 (t, ^1J(C,P) = 13.4 Hz, CH_2P), 58.3 (s, CH_3CH_2O), 128 (t, ^1J(C,P) = 5.1 Hz, phenyl ring), 128.3 (t, ^1J(C,P) = 5.1 Hz, phenyl ring), 130.2 (s, phenyl ring), 133.7 (t, ^1J(C,P) = 5.9 Hz, phenyl ring); elemental analysis calcd (%) for $C_{40}H_{58}Cl_2O_6P_2PdSi_2$: Pd 11.44, P 6.66; found: Pd 11.7, P 6.04.

2.1.2. Bis{(dicyclohexylphosphino) propyltriethoxysilane)}palladium dichloride, 2

Yield: 85% as yellow crystals; ^{31}P {^1H} NMR (81 MHz, $CDCl_3$, 25 °C) δ 22 (s); ^{13}C NMR (50 MHz, $CDCl_3$, 25 °C) δ 12.7 (t, ^3J(C,P) = 6.4 Hz, CH_2Si), 18.25 (s, CH_3CH_2O), 19.04 (s, $CH_2CH_2CH_2Si$), 21.96 (t, ^1J(C,P) = 10.2 Hz, CH_2P), 26.35 (s, C_p), 27.13 (t, ^3J(C,P) = 5.3 Hz, C_m), 27.44 (t, ^3J(C,P) = 5.9 Hz, C_m), 28.7 (brs, C_o), 29.3 (brs, C_o), 32.8 (t, ^{1}J(C,P) = 11.2 Hz, C_i), 58.3 (s, CH_3CH_2O); elemental analysis calcd (%) for $C_{42}H_{86}Cl_2O_6P_2PdSi_2$: Pd 10.83, P 6.30; found: Pd 9.9, P 6.33.

2.1.3. {Bis[(diphenylphosphanyl)methyl]amino} propyltriethoxysilanepalladium dichloride, 3

Yield: 99% as greenish solid; ^{31}P {^1H} NMR (81 MHz, $CDCl_3$, 25 °C) δ 7 (s); ^{13}C NMR (50 MHz, $CDCl_3$, 25 °C) δ 7.6 (s, CH_2Si), 18.2 (s, CH_3CH_2O), 18.6 (s, $CH_2CH_2CH_2Si$), 56 and 57 (dd, ^1J(C,P) = 2.3 Hz and ^3J(C,P) = 47 Hz, NCH_2P), 58.4 (s, CH_3CH_2O), 65 (t, ^3J(C,P) = 10 Hz, $NCH_2CH_2CH_2$), 128.2–134 (phenyl carbons); elemental analysis calcd (%) for $C_{35}H_{45}Cl_2NO_3P_2PdSi$: Pd 13.4, P 7.8; found: Pd 13, P 7.5.

2.2. Synthesis of palladium mesoporous silica materials

The covalent immobilization of palladium complexes was performed using a post-synthesis procedure by directly reacting the alkoxysilane moieties of the phosphine (or cyano) ligand with surface silanols of a surfactant-free mesoporous oxide. Mesoporous SBA-15 type silica was used as support and was prepared by the acid catalyzed, non-ionic assembly pathway described elsewhere [28,29]. The structure directing agent (Pluronic 123) was removed quantitatively from the as-synthesized material by calcination at 500 °C overnight under air as evidenced by TGA analysis and infrared spectroscopy. Prior to the grafting reaction, the surfactant-free mesoporous silica was rigorously dried under vacuum at 160 °C. Palladium complexes 1–4 (1.6 mmol) dissolved in 20 mL of deaerated toluene were then added to a suspension of SBA-15 silica (2 g) in dry toluene. The reaction mixture was first stirred at 25 °C for 6 h to allow the diffusion of the molecular precursor into the channels of the pores, then heated overnight at temperatures ranging from 50 to 80 °C depending on the stability of the palladium precursor. The resulting solid was filtered under nitrogen, washed thoroughly with small amount of toluene and finally dried at 30 °C under vacuum.

[1]@SBA-15: ^{13}C CP-MAS NMR δ 7.9, 17.4, 21, 59, 129; ^{29}Si CP-MAS NMR δ −44.7, −51.6, −99.5, −106; ^{31}P CP-MAS NMR δ 22.9, 34.4; elemental analysis (wt%): Pd 3.06, P 1.88, Cl 2.12.

[2]@SBA-15: ^{13}C CP-MAS NMR δ 12, 20.7, 27.2, 59.5; ^{29}Si CP-MAS NMR δ −36.3, −41, −91.5, −98.4, −104.6; ^{31}P CP-MAS NMR δ 23.8; elemental analysis (wt%): Pd 1.2, P 0.80, Cl 0.8.

[3]@SBA-15: ^{13}C CP-MAS NMR δ 8.2, 17.4, 25.8, 58.9, 129.4; ^{29}Si CP-MAS NMR δ −38.5, −41, −86.4, −99.2, −104.6; ^{31}P CP-MAS NMR δ 11.7; elemental analysis (wt%): Pd 3.8, P 2.30, Cl 2.69, N 0.65.

[4]@SBA-15: ^{29}Si CP-MAS NMR δ −46.7, −56, −65.1, −88.9, −98.1, −105.7; elemental analysis (wt%): Pd 1.75, N 0.42.

2.3. Catalysis

2.3.1. Catalytic procedure

The heteroannulation of 2-iodoaniline with triethyl (phenylethynyl)silane was chosen as a benchmark reaction to evaluate the performance of the palladium hybrid materials. The catalytic reaction was carried out under an argon atmosphere in a two-necked flask fitted with argon inlet and a septum allowing direct sampling of the reaction mixture under argon flow. In a typical procedure, the hybrid catalyst (1 mol% of Pd based on elemental analysis) was first evacuated at 40 °C during 4 h to remove physisorbed water and then suspended in 4 mL DMF followed by addition of 2-iodoaniline (1 mmol), triethyl(phenylethynyl)silane (3 mmol) and Na_2CO_3 (3 mmol). The reactor was placed under stirring in a preheated oil bath at 120 °C. The advancement of the reaction was monitored by GC–MS. After cooling at room temperature, the reaction mixture was filtered through a pad of celite, which was washed with EtOAc (100 mL). The resulting organic layer was then washed with Na_2CO_3 (2× 40 mL) and brine (40 mL) and finally dried over Na_2SO_4. After removal of the solvent under reduced pressure, the crude product was fully deprotected according to the previously reported method [27] before being purified by flash chromatography over silica (petroleum ether/methylene chloride 9:1). 3-phenyl-1*H*-indole was obtained as a white solid in 80–85% yield depending on the catalytic solid involved in the reaction. Data obtained are in accordance with the literature.

mp 85–87 °C; νmax (KBr): 3410, 3390, 3055, 3035, 2925, 1538, 1486, 1338 cm^{-1}; ^1H NMR (250 MHz, $CDCl_3$) δ 8.07 (brs, 1H), 8.00 (d, J = 7.4 Hz, 1H), 7.71 (dd, J = 8.2, 1.0 Hz, 2H), 7.49 (t, J = 7.4 Hz, 2H), 7.44–7.18 (m, 5H); ^{13}C NMR (63 MHz, $CDCl_3$) δ 136.6 (C), 135.5 (C), 128.7 (CH), 127.4 (CH), 125.9 (CH), 125.6 (C), 122.3 (CH), 121.8 (CH), 120.3 (CH), 119.7 (CH), 118.2 (C), 111.4 (CH).

2.3.2. Leaching procedure

Leaching studies were performed using the hot-filtration technique. After 10–40 min reaction of a standard catalytic run, the supernatant solution was filtered at 120 °C through a hot cannula with a microglass Whatman filter (in order to remove all fine particles). Then, the inorganic base (3 equiv.) filtered by part was added and the mixture treated for further 6–15 h under standard reaction conditions. The reaction was monitored over the total period by GC and the results compared to a standard catalytic reaction.

2.3.3. Recycling procedure (multi-run experiments)

In the recycling studies, the catalyst activity was examined two times (at 2 and 14 h reaction time) by check-up of conversion. In a typical experiment, fresh catalyst was used as for a standard catalytic run. After 24 h reaction new amounts of reagents (1 mmol of 2-iodoaniline, 3 mmol of triethyl(phenylethynyl)silane and 3 mmol of Na_2CO_3) were added. The volume of solvent was adjusted in order to restore the concentrations of reagents to that of the initial run. Immediately after addition, based on GC analysis, the concentration of the 2-iodoaniline was considered as 100% and the concentration in 3-phenyl-2-(triethylsilyl)-1*H*-indole to 0%. The reaction was followed by GC for another 24 h and the procedure was repeated four times.

3. Results and discussion

3.1. Preparation of palladium mesoporous silica materials

Heterogeneous catalyst synthesis was achieved through the covalent immobilization of palladium-based complexes on the surface of preformed mesoporous SBA-15 type silica. SBA-15 silica represents one of the most attractive host materials for the immobilization of catalytically relevant species owing to its large

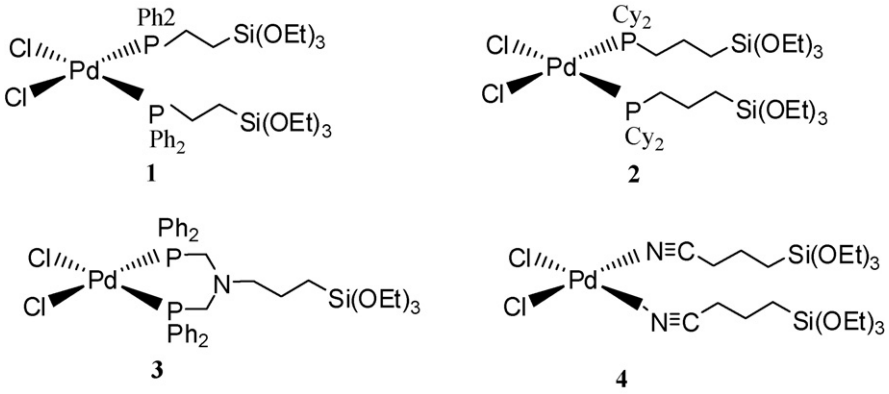

Scheme 1. .

pore volume and diameter (up to 80 Å) which allow for better reactant and product diffusion, hence reducing mass transfer limitations and allowing even large molecules to access the catalytic sites. In addition, SBA-15 possesses thick walls providing thermal and hydrothermal stability which may be a key factor for recycling experiments [28,29]. The covalent link to the silica surface was introduced through the ligands coordinated to the metal centre which implied the use of bifunctional molecules bearing on one side polycondensable organosiloxane precursor moiety and on the other end functional group such as phosphine or nitrile able to bind the metal site. Four different palladium (II) complexes of the general formula $PdCl_2L_2$ were considered (Scheme 1). The simplest ligand tested was the commercial 2-(diphenylphosphino)ethyltriethoxysilane which after coordination led to a palladium complex 1 bearing two monodentate phosphine linkers. A saturated analog of this ligand (cyclohexyl in place of phenyl, complex 2) provides a ligand system which is both more electron-rich and more sterically hindered. The chelating diphosphine $(EtO)_3SiCH_2CH_2CH_2N(CH_2PPh_2)_2$, which should provide a stronger metal–ligand bonding, and its corresponding palladium complex 3 were prepared to gain insight into the effect of chelation on catalyst performance and stability toward leaching. Finally, a commercial, phosphine-free ligand $(EtO)_3SiCH_2CH_2CH_2CN$ was tested affording an ethoxysilane-modified version of $PdCl_2$ (complex 4), particularly interesting for applications under oxidizing conditions which render phosphine-based systems unstable.

The covalent grafting of palladium complexes 1–4 onto organic-free SBA-15 silica was carried out in degassed toluene at temperatures ranging from 50 to 80 °C depending on the stability of the palladium precursor. The unreacted palladium complexes were removed by thorough washing the solid with toluene and methylene chloride leading to hybrid Pd materials referred to as [*X*]@SBA-15 with *X* = 1–4. Several methods were used to characterize the molecular and bulk properties of the catalytic solids: X-ray powder diffraction (XRD) at small and wide angles, transmission electron microscopy (with EDX), elemental analysis, thermogravimetric analysis, infrared spectroscopy, multi-nuclear NMR spectroscopy and nitrogen sorptions. The physicochemical properties of the hybrid materials derived from the powder XRD and sorption analyses are summarized in Table 1. Typical XRD patterns of the hybrid materials are shown in Fig. 2. All the palladium modified solids exhibited typical diffractograms characteristic of hexagonally ordered mesophases with the presence of three well resolved peaks in the 2θ-range of 0.6°–3° attributed respectively to the (1 0 0), (1 1 0) and (2 0 0) reflexions. The presence of higher order reflexions indicates that the chemical bonding procedure

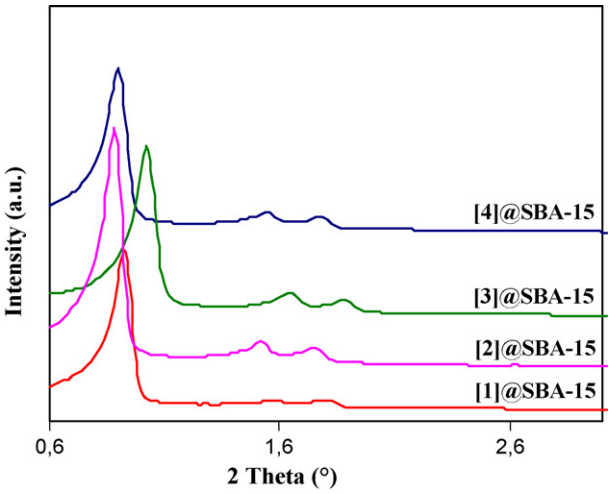

Fig. 2. X-ray powder diffraction patterns of SBA-15 mesoporous materials after grafting of palladium precursors.

Table 1
Physical and textural properties of palladium containing hybrid silica materials.

Catalyst	Pd (%$_{wt}$)	d_{100}[a] (Å)	a_0[b] (Å)	Wall thickness[c] (Å)	V_p[d] (cm^3 g^{-1})	D_p[e] (Å)	S_{BET} (m^2 g^{-1})	C_{BET}
[1]@SBA-15	3.06	96	111	57	0.66	54	601	181
[2]@SBA-15	1.2	100	115	52	0.80	63	553	114
[3]@SBA-15	3.8	105	121	63	0.53	58	367	110
[4]@SBA-15	1.75	98	113	50	0.87	63	644	122

Different batches of bare SBA-15 silica were used to construct the various catalysts and their physical and textural properties are summarized in Supplementary Material (Table S1).

[a] $d(100)$ spacing.
[b] $a_0 = 2d(100)/\sqrt{3}$, hexagonal lattice parameter calculated from XRD.
[c] Calculated by a_0 – pore size.
[d] Total pore volume at $P/P0 = 0.980$.
[e] Pore size from desorption branch applying the BJH pore analysis.

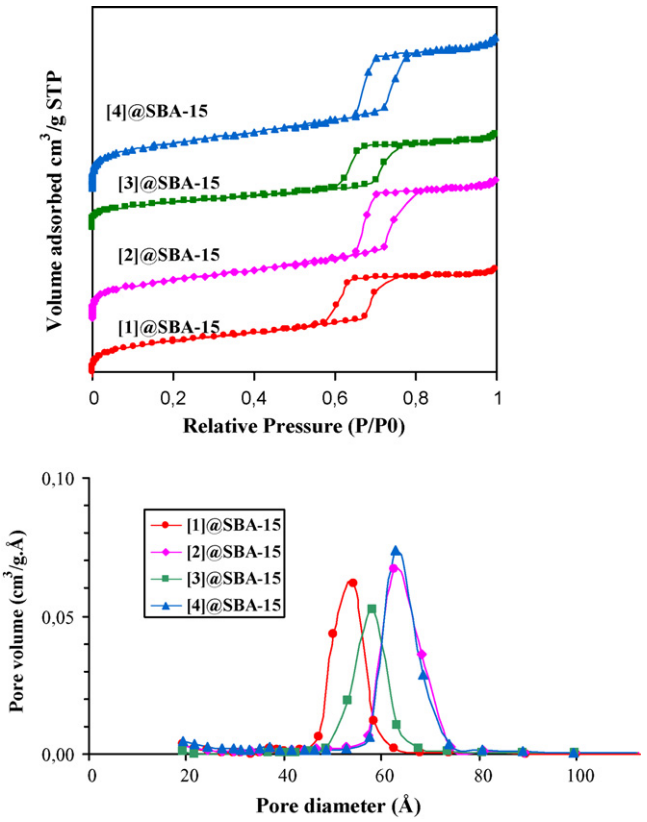

Fig. 3. Nitrogen adsorption/desorption isotherms (top) and pore size distribution (bottom) of palladium functionalized SBA-15 silica materials.

did not diminish the long-range structural ordering of the materials. *d* spacings ranging from 105 to 96 Å were determined for the grafted samples which corresponds to unit-cell parameters varying between 121 and 111 Å. An increase in the unit-cell parameters of the hybrids compared to the parent silicas was generally observed which could stem from a change in wall thickness and/or modification of the pore size (*vide infra*) (Supplementary Material, Table S1).

Nitrogen adsorption–desorption measurements were used to examine the textural properties of the hybrid materials. Typical isotherms and pore size distributions are depicted in Fig. 3. All the materials exhibited type IV isotherms and H1 hysteresis loops characteristic of mesoporous solids and SBA architectures. A steep capillary condensation step appearing at relative pressure of $P/P0 = 0.6–0.8$ (Fig. 3, top) indicated the presence of regular mesopores in the samples which was confirmed by a narrow pore size distribution in the mesopore range (Fig. 3, bottom). High BET surface areas (367–644 $m^2\,g^{-1}$) were obtained for all the samples upon functionalization with average pore diameters and pore volumes varying respectively between 54 and 63 Å and 0.53 and 0.87 $cm^3\,g^{-1}$. It is worth noting that significant decreases in specific surface areas, pore diameters and pore volumes compared to parent SBA-15 silicas (Supplementary Material, Table S1) were observed for almost all the solids after functionalization with the exception of (3-cyanopropyltriethoxysilane) palladium dichloride modified solid, [4]@SBA-15, for which only a slight decrease in surface area was noticed (from 704 $m^2\,g^{-1}$ for plain SBA-15 to 644 $m^2\,g^{-1}$ after grafting). Also, it is interesting to mention that, in the case of organophosphine palladium complexes modified materials, the decrease in pore size was accompanied by a significant increase in the wall thickness (from 34–45 Å to 52–63 Å). Taken together, these observations are consistent with the presence of a significant amount of grafted palladium species attached to the internal surface of the mesopores.

Solid-state ^{29}Si NMR spectroscopy provided further information about the nature of the link to the surface, the silicon environment and the degree of functionalization. The ^{29}Si CP-MAS NMR spectra of SBA-15 mesoporous materials after grafting of palladium precursors 1–4 (Fig. 4) displayed discernable peaks in two different spectral regions: one region ranging from −95 to −110 ppm characteristic of *Q*-type ($Q^n = Si–(OSi)_n–(OH)_{4-n}$) silicates originating from the siliceous bulk material and another set of signals appearing in the −40 to −80 ppm spectral region ascribed to *T*-type ($T^m = RSi–(OSi)_m–(OH)_{3-m}$) silicates, that is, the silicon atoms attached to the phosphine and/or cyano containing alkyl chain which is a clear indication of covalent bonding. Note that multiple peaks were obtained from each of the modified oxides, suggesting different degrees of linkage of the organosiloxane group with the silica surface. All four modified oxides exhibited principally T^1 and T^2 sites, that is, an anchoring of the organic species via one or two Si–O–Si bonds. In the case of palladium complexes bearing monophosphine ligands, [1]@SBA-15 and [2]@SBA-15, the absence of T^0 sites seems to suggest that both phosphine linkers were involved, at least, in one covalent bond with the support resulting in chelation through the silica surface.

Examination of the ^{13}C CP-MAS NMR spectra of the palladium modified solids along with the solution phase spectra of the corresponding molecular precursors 1–3 (Supplementary Material, Figs. S1–S3) led to the conclusion that the structure of the organic fragments (mainly the ligands coordinated to the metal centre) in the grafted solids remained intact throughout the functionalization process. One should also note the occurrence, in all three spectra, of two resonances corresponding to unreacted alkoxysilane groups ($\delta = 17$ and 58 ppm) indicating the presence of residual ethoxy groups at the point of attachment with the surface, which is also consistent with the presence of not fully condensed T^1 and T^2 sites.

Solid-state ^{31}P NMR spectroscopy proved to be a useful technique to elucidate the structural integrity and coordination mode of the phosphine linkers at the palladium centre in the supported complexes. The ^{31}P CP-MAS NMR spectra of the modified SBA-15 silica materials are presented in Supplementary Material (Figs. S4–S6) together with the liquid ^{31}P NMR of their respective molecular precursors 1–3. In all cases, the Pd–P bond seemed unaffected by grafting: free ligands were not detected (negative δ expected at higher magnetic field) and the ^{31}P NMR chemical shifts present in the spectra of the grafted materials correspond to coordinated phosphine ligands (see Section 2 for numerical values). As expected for heterogenized species, a relatively broad signal centred at 23.8

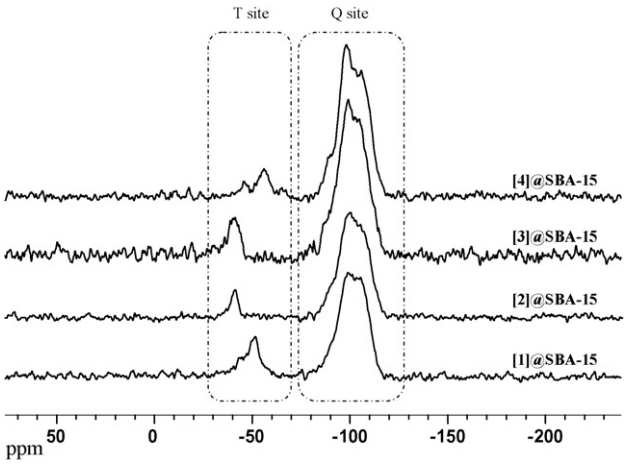

Fig. 4. CP-MAS ^{29}Si NMR of SBA-15 mesoporous materials after grafting of palladium precursors.

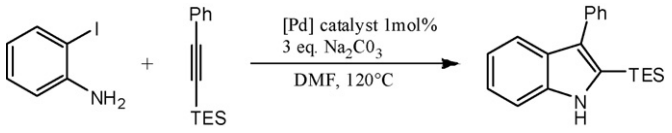

Scheme 2. .

and 11.7 ppm was observed for respectively [2]@SBA-15 (Fig. S5) and [3]@SBA-15 (Fig. S6). In the case of [1]@SBA-15 (Fig. S4) one may discern the presence of two resonances at $\delta = 22.9$ and 34.4 ppm, which can be assigned to respectively the *trans*- and *cis*-isomers of the grafted species (the liquid NMR spectrum of the molecular precursor 1 showed two peaks at $\delta = 21.4$ and 31.7 ppm). This result clearly indicates that the monophosphine ligands have survived the grafting reaction and are still coordinated by pairs to the palladium central atom.

Quantitative determinations of metal and organic contents were performed for all the hybrid materials by thermogravimetric analysis (TG/DTG) in air and elemental analysis. Generally, similar thermal profiles were observed for all the hybrids, composed of three weight loss regions (Supplementary Material, Fig. S7). A first weight loss occurred at temperatures up to about 200 °C and was assigned to the desorption of physisorbed water. A second weight loss occurred at temperatures ranging from 200 to 600 °C presumably arising from the decomposition of organic species. Depending on the nature of the organic fragments, several desorption peaks could be observed in this region with weight losses ranging from 4.6 to 16.6%$_{wt}$ (Supplementary Material, Table S2). Note that the first decomposition peak occurs at relatively elevated temperature (~280 °C) revealing the high thermal stability of the palladium immobilized materials regardless the nature of the coordinated ligands. The third weight loss region, which took place above 600 °C, was ascribed to the release of water formed from the condensation of silanols in the silica structure. In quantitative terms, one should consider the organic loading of the surface in comparison to the dry mineral weight of the material, in this case, the weight of the material at the end of thermal treatment. Thus, the functional group loading in the grafted palladium solids was found to be in the range of 0.05–0.21 g/g of dry SiO_2 as determined by TGA (Supplementary Material, Table S2). Elemental analyses of palladium, phosphorus, chlorine and nitrogen obtained for the palladium containing hybrid materials are summarized in Table S3 (Supplementary Material). In general, upon functionalization, palladium content was found to vary between 1.2 and 3.8%$_{wt}$ in the hybrid solids. In the case of materials functionalized with organophosphine palladium complexes, a phosphorus/palladium molar ratio of 2.1–2.3 (expected 2) and a chlorine/palladium molar ratio of 2–2.1 (expected 2) were found indicating that on average two phosphorus and two chlorine atoms per palladium centre were left on the surface. This suggests that the stoichiometry of the initial molecular precursors 1–3 was not affected by the grafting procedure. In the case of [4]@SBA-15, which contains weakly coordinative cyano ligands, the integrity of the molecular precursor 4 was also maintained with a nitrogen/palladium molar ratio of 1.8 (expected 2).

3.2. Palladium catalyzed Larock indole synthesis

These catalytic materials, [1]–[4]@SBA-15, were applied to Larock indole synthesis (Scheme 2) using optimized reaction conditions previously described for Pd[$(NH_3)_4$]/NaY and Pd/C (i.e. 2-iodoaniline (1.0 mmol), alkyne (3.0 mmol), Na_2CO_3 (3 mmol), [Pd] catalyst (1 mol%), DMF (4.0 mL), 120 °C) [27]. Initially, catalysts [1]–[4]@SBA-15 were evaluated for the synthesis of 3-phenyl-2-(triethylsilyl)-1*H*-indole over a period of 24 h; in all cases isolated yields of 80–85% were achieved.

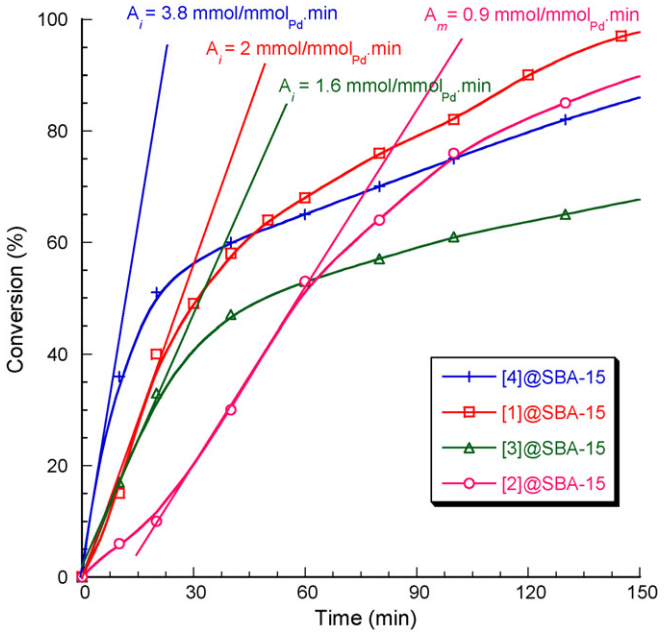

Fig. 5. Catalytic activity of palladium mesoporous SBA-15 silica materials in the heteroannulation of 2-iodoaniline with triethyl(phenylethynyl)silane.

More insights were obtained from kinetic studies (Fig. 5). Except for the cyclohexylphosphine-based catalyst [2]@SBA-15 all show clearly high activities for the studied reaction as determined from initial rates: 3.8 mmol mmol$_{Pd}^{-1}$ min^{-1} for the cyano catalyst [4]@SBA-15, 2.0 mmol mmol$_{Pd}^{-1}$ min^{-1} for the monodentate diphenylphosphine-based catalyst [1]@SBA-15 and 1.6 mmol mmol$_{Pd}^{-1}$ min^{-1} for the chelated diphosphino catalyst [3]@SBA-15. Interestingly, all these materials show higher activities than the previously evaluated catalysts; Pd/C (0.5 mmol mmol$_{Pd}^{-1}$ min^{-1}) and Pd/NaY (1.3 mmol mmol$_{Pd}^{-1}$ min^{-1}) (Supplementary Material, Fig. S8). Surprisingly, the curve obtained for the cyclohexylphosphine-based catalyst [2]@SBA-15 showed an inflexion point at *ca.* 20 min probably related to a modification in the nature of the supported palladium species. While the initial rate arises only 0.3 mmol mmol$_{Pd}^{-1}$ min^{-1}, the activity reached after this point 0.9 mmol mmol$_{Pd}^{-1}$ min^{-1}. However, further studies were not performed with this catalyst due to its lower activity in comparison to that achieved with the other materials evaluated in the present contribution.

When heterogeneous materials are used in liquid phase, questions regarding leaching and recycling should be addressed. These issues were addressed for the two most promising catalysts, namely [1]@SBA-15 and [4]@SBA-15. Leaching is almost often observed when supported palladium catalysts are used in such cross-coupling reactions [23,30]. Several methodologies are commonly used [23,31], the hot-filtration method, when applied with care, provides quick and reliable information about leaching. The procedure (see Section 2) was applied to [1]@SBA-15 after 20 min reaction corresponding to *ca.* 40% conversion and after 10 min (33% conversion) for [4]@SBA-15. Comparing a standard run (in the presence of solid material) to the hot-filtration run (Fig. 6) clearly showed further product formation after removal of the heterogeneous catalyst, up to a conversion of 80% after 6 h for [1]@SBA-15 and 75% after 6.5 h for [4]@SBA-15. These data clearly indicate that active palladium species are dissolved during the reaction. The differences in performances observed between the runs with and without the solid material can be related to: (1) the lack of continuous palladium source due to the removal of the material; (2)

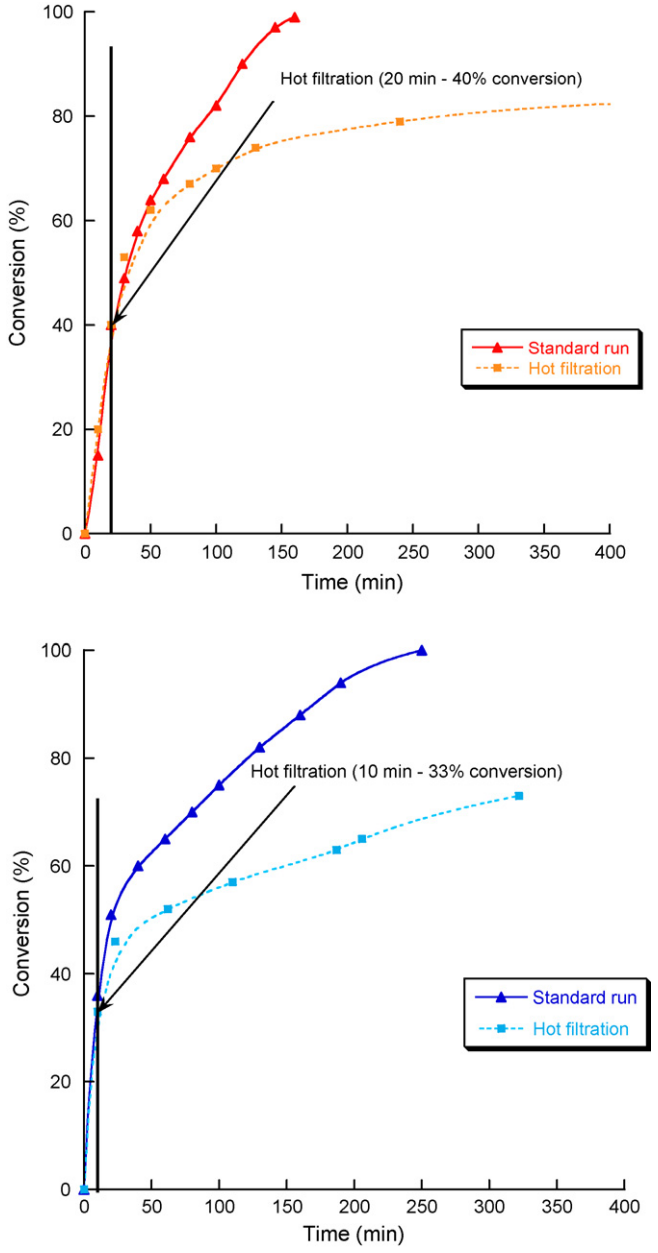

Fig. 6. Residual activity of [1]@SBA-15 (top) and [4]@SBA-15 (bottom) after hot filtration (dotted line) versus standard catalytic run (solid line).

deactivation of the dissolved palladium species to less active colloids or palladium black; or (3) to the removal of the contribution of a heterogeneous catalysis to the overall conversion (which we consider as an unlikely or very minor factor) [23].

For each of the leaching experiments, the transparent, colourless solution was analyzed by AAS and found to contain palladium. The values ranged from 14 to 32 ppm are reported in Table S4 of the Supplementary Material. It should be noted that these concentrations are below the acceptable standards under European regulations for residual palladium content administered by oral and parental routes in drug testing, and thus the products could be used without further purifications (in regard to palladium content), a clear advantage for such a heterogeneous system [32].

Recycling of the catalyst [1]@SBA-15 and [4]@SBA-15 was initially performed by separating the solid material from the reaction mixture by filtration to afford a *used* catalyst that was recycled after washing in a further run. The results thus obtained showed a strong deactivation that could not be fully related to mass loss.

This phenomenon was further studied through multi-run experiments, with analysis of each cycle performed both early and later in the cycle. This study was carried out on the two most highly performing catalysts, the cyano catalyst [4]@SBA-15 and the monodentate diphenylphosphine-based catalyst [1]@SBA-15. In each series, a first run was performed using fresh catalyst for 24 h. Aliquots were removed after 2 and 14 h of reaction and analyzed by GC. At this point, a new portion of the reagent mixture was added (1 mmol of 2-iodoaniline, 3 mmol of triethyl(phenylethynyl)silane and 3 mmol of Na_2CO_3) and the volume of solvent was adjusted in order to restore the concentrations of reagents to that of the initial run. The reaction was then allowed to proceed an additional 24 h, aliquots being withdrawn and analyzed 2 and 14 h after the addition of reactants. The process was repeated to a total of five fixed time reaction cycles.

Data obtained in the short run study (Fig. 7, left) confirm deactivation of the catalysts from initially moderate (i.e. 30% for the 2nd run) to low conversions (i.e. 17–9% for the 3rd to 5th runs). Differences between the two catalysts were observed: while the activity of [4]@SBA-15 continuously decreased, that of [1]@SBA-15 remained constant after the 3rd run (stabilized at *ca.* 14%). The long run study (Fig. 7, right) shows that despite the lower initial activity implied by the short run study, the catalyst system remains viable over the five runs. That is, as one can observe in Fig. 7, quantitative conversion to the expected product is observed for every run when the 14 h reaction time was used, making these materials particularly efficient for such applications.

To further explore the origin of observed deactivation, used catalysts were analyzed by X-ray diffractometry and electron microscopy (including EDX). Specifically, for catalysts [1]@SBA-15 and [4]@SBA-15, data were obtained for fresh catalyst and catalyst recovered after a single 14 h run. The latter catalysts were filtered and washed with water and DMF to remove the salts (NaI and $NaHCO_3$) formed during the reaction.

Small angle XRD analysis for all samples indicated long-range mesoscopic ordering, indicating that no wholesale collapse of the mesostructure occurred over five runs (Figs. S9 and S10) even though, in some cases, decrease in intensity of the d_{100} reflection was observed (ascribed mainly to lower local ordered regions). In the wide-angle XRD patterns (Fig. S11), none of the samples displayed the characteristic diffraction pattern of crystalline palladium phase, indicating that no significant sintering occurred.

Electron microscopy was shown to be destructive for the cyano palladium catalyst, [4]@SBA-15.[1] In the TEM imagery as illustrated for [1]@SBA-15 (Fig. 8), long-range ordering was also clearly evident for each of the three samples. The TEM/EDX data (Table 2) for the fresh catalyst showed that palladium was uniformly localized in well ordered phases of the solid and the ligand to metal ratio (i.e. the P/Pd ratio) of the molecular precursor 1 was confirmed (1.9 for an expected value of 2.0). This observation was confirmed over a multiple sample areas of the surface of each of the materials tested. Note that the elemental analysis of a milligram scale sample of [1]@SBA-15 also showed a phosphorous/palladium ratio of 2.1.

Microscopy of the used catalysts showed no gross changes in the structure of the mesoporous silica networks, and notably, no formation of large palladium particles. Analysis of the used sam-

[1] The TEM images of [4]@SBA-15, including the fresh catalyst, showed the expected hexagonal channels of the SBA-15 with the presence of large palladium particles and aggregates. This result, particularly for the fresh catalyst, is inconsistent with elemental analyses. We undertook an XPS study in order to ascertain palladium oxidation state in the fresh material. One was able to observe visually the solid sample turning from white to black at the point of contact with the XPS beam.

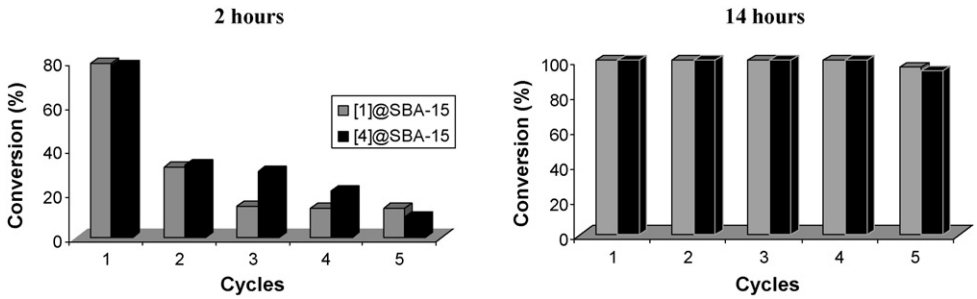

Fig. 7. Recyclability of [1]@SBA-15 and [4]@SBA-15 for the heteroannulation of 2-iodoaniline with triethyl(phenylethynyl)silane examined at 2 h (left) and 14 h (right).

ples (Table 2), however, showed progressive loss of palladium upon recycling, with no palladium detected in the three sites sampled after the fifth run of the catalysts.

All results clearly indicate palladium loss upon recycling procedures. However, from our "in situ" recycling experiments we demonstrated that the material still features good activity when not removed from the reaction mixture. This suggests that for some reason the leached palladium did not efficiently redeposit on the support, which may be attributed to several factors. One hypothesis would be that the material surface is not adapted to accommodating or stabilizing the palladium after leaching, thus preventing effective redeposition. Given the nature of the support

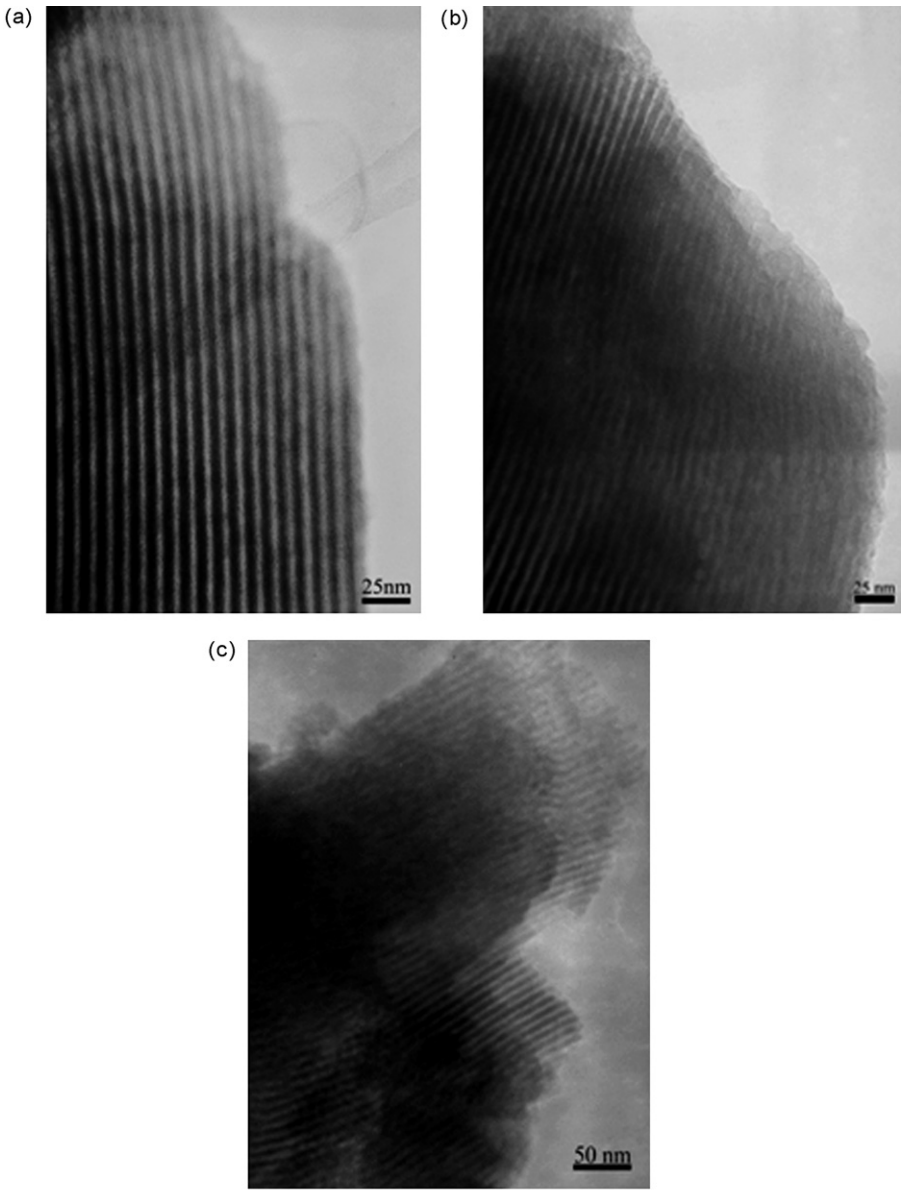

Fig. 8. TEM micrographs in the direction perpendicular to the pore axis of [1]@SBA-15: (a) fresh catalyst; (b) after the 1st cycle; and (c) after the 5th cycle.

Table 2
TEM/EDX analysis on [1]@SBA-15 samples (fresh catalyst and single run).

Catalyst	EDX sample[a]	Atom counts			P/Pd
		Si	P	Pd[b]	
fresh [1]@SBA-15	1	100	4.13	2.25	1.83
	2	100	4.57	2.68	1.7
	3	100	4.77	2.33	2.04
	Average	100	4.49	2.42	1.85
[1]@SBA-15 after one 14-h run	1	100	3.59	0.90	3.98
	2	100	3.23	0.80	4.03
	3	100	3.28	0.76	4.31
	Average	100	3.37	0.82	4.1

[a] Measurements taken at different locations on the sample.
[b] From the milligram scale microanalysis, one would expect 1.72 atoms Pd per 100 atoms Si.

and its large surface area, we can very probably discard this hypothesis. Alternatively, it could be that the palladium redeposition is prevented by the large amount of salts present in the solution (about 450 mg of sodium salts are produced in each run, or approximately 2.3 g after 5 runs, compared to 35–65 mg of Pd-catalyst). These salts probably crystallize upon cooling (and probably during the reaction) with two concomitant effects: (a) salt crystallization encapsulates leached palladium which was then eliminated when the solid was washed with water and DMF prior to XRD and TEM studies; (b) salt crystallization can occur at the pore mouth of the SBA-15 material preventing effective palladium redeposition by reducing the accessibility to the large internal support surface area.

To date, we cannot with certitude discard one or the other hypothesis; however we strongly support the second one as this was previously observed with other microporous supports like NaY zeolites that has already proven its capacity to accommodate leached palladium toward efficient recycling in common cross-coupling reactions [9].

As the main purpose of this work was to propose catalytic systems with overall high performance, especially relative to homogeneous state of the art, we have not prioritized the study of this process, but specific experiments toward better understanding are currently under way in order to optimize catalyst design toward higher recycling.

Given the efficiency of these materials, we undertook other studies on the much more challenging Larock synthesis from bromoaniline for which the sole examples described in homogenous media involved the use of costly hindered phosphine or urea ligands [33,34]. In initial experiments we performed the first "salt-free" heterogeneously palladium catalyzed Larock reaction between the 2-bromoaniline with the triethyl(phenylethynyl)silane that gave for all materials described in this contribution the expected indole in high isolated yields (up to 85%).

4. Conclusion

A series of palladium containing mesostructured hybrid materials have been prepared and fully characterized by several techniques. All analyses performed demonstrated that the preparation methodology allowed effective immobilization of preformed palladium complexes without affecting the integrity of the complexes.

These materials offer viable alternatives to the use of homogeneous catalytic systems for the Larock synthesis of indoles as they proved to be robust, capable of quantitatively converting iodoaniline toward the target compounds and to be recyclable through multiple recycling experiments. The detailed and comprehensive studies of the catalytic phenomena showed it to be homogeneous in nature, the solid apparently serving as "continuous source" of palladium between cycles, that is, as a catalyst reservoir.

Current work concentrates on optimization of the palladium hybrid materials toward higher recycling capacities and on the extension of the Larock indole syntheses to a variety of bromoanilines.

Acknowledgements

The authors gratefully acknowledge the Région Rhône-Alpes Programme CIBLE-2007 (Contract number 07 016376 01/02/03) and the National Agency of Research (No. ANR-07-BLAN-0167-01/02) for funding. NB thanks Région Rhône-Alpes for a grant. AB thanks ANR for felowship. The authors kindly acknowledge the "Technical Center" of IRCELYON for analyses and helpful discussions (M. Aouine and L. Burel for TEM, P. Mascunan and N. Cristin for AAS analyses, P. Delichère and S. Prakash for XPS, F. Bosselet and G. Bergeret for XRD and C. Lorentz for solid-state NMR).

Appendix A. Supplementary data

Supplementary data associated with this article can be found, in the online version, at doi:10.1016/j.apcata.2010.08.046.

References

[1] J.A. Joule (Ed.), Product Class 13: Indole and Its Derivatives, Thieme, Stuttgart, 2001.
[2] R.J. Sundberg, Indoles, Academic Press, London, 1996.
[3] L. Joucla, L. Djakovitch, Adv. Synth. Catal. 351 (2009) 673–714.
[4] B. Robinson, The Fischer Indole Synthesis, John Wiley & Sons, Chichester, 1982.
[5] R.J. Sundberg (Ed.), Pyrroles and their Benzo Derivatives: Synthesis and Applications, Pergamon, Oxford, 1984.
[6] J. Tois, R. Franzén, A. Koskinen, Tetrahedron 59 (2003) 5395–5405.
[7] G. Battistuzzi, S. Cacchi, G. Fabrizi, Eur. J. Org. Chem. (2002) 2671–2681.
[8] S. Cacchi, G. Fabrizi, Chem. Rev. 105 (2005) 2873–2920.
[9] S. Chouzier, M. Gruber, L. Djakovitch, J. Mol. Catal. A: Chem. 212 (2004) 43–52.
[10] G. Cusati, L. Djakovitch, Tetrahedron Lett. 49 (2008) 2499.
[11] L. Djakovitch, V. Dufaud, R. Zaidi, Adv. Synth. Catal. 348 (2006) 715–724.
[12] L. Djakovitch, P. Rollet, Adv. Synth. Catal. 346 (2004) 1782–1792.
[13] L. Djakovitch, P. Rouge, J. Mol. Catal. A: Chem. 273 (2007) 230–239.
[14] L. Djakovitch, P. Rouge, Catal. Today 140 (2009) 90–99.
[15] L. Djakovitch, P. Rouge, R. Zaidi, Catal. Commun. 8 (2007) 1561–1566.
[16] M. Gruber, S. Chouzier, K. Koehler, L. Djakovitch, Appl. Catal. A: Gen. 265 (2004) 161–169.
[17] G. Huang, R.C. Larock, J. Org. Chem. 68 (2003) 7342–7349.
[18] R.C. Larock, S. Babu, Tetrahedron Lett. 28 (1987) 5291–5294.
[19] R.C. Larock, S. Babu, Tetrahedron Lett. 28 (1987) 1037.
[20] R.C. Larock, E.K. Yum, J. Am. Chem. Soc. 113 (1991) 6689–6690.
[21] R.C. Larock, E.K. Yum, M.D. Refvik, J. Org. Chem. 63 (1998) 7652–7662.
[22] G. Zeni, R.C. Larock, Chem. Rev. 106 (2006) 4644–4680.
[23] L. Djakovitch, K. Koehler, J.G. De Vries, in: D. Astruc (Ed.), Nanoparticles and Catalysis, Wiley-VCH, Weinheim, 2008, pp. 303–348.
[24] F.-X. Felpin, E. Fouquet, ChemSusChem 1 (2008) 718–724.
[25] F.-X. Felpin, O. Ibarguren, L. Nassar-Hardy, E. Fouquet, J. Org. Chem. 74 (2009) 1349–1352.
[26] L.X. Yin, J. Liebscher, Chem. Rev. 107 (2006) 133–173.
[27] N. Batail, A. Bendjeriou, T. Lomberget, R. Barret, V. Dufaud, L. Djakovitch, Adv. Synth. Catal. 351 (2009) 2055–2062.
[28] D. Zhao, J. Feng, Q. Huo, N. Melosh, G.H. Fredrickson, B.F. Chmelka, G.D. Stucky, Science 279 (1998) 548–552.
[29] D. Zhao, Q. Huo, J. Feng, B.F. Chmelka, G.D. Stucky, J. Am. Chem. Soc. 120 (1998) 6024–6036.
[30] N.T.S. Phan, M. Van Der Sluys, C.W. Jones, Adv. Synth. Catal. 348 (2006) 609–679.
[31] J.M. Richardson, C.W. Jones, J. Catal. 251 (2007) 80–93.
[32] European Medicines Agency, in: E.M. Agency (Ed.), 2008, p. 34.
[33] X. Cui, J. Li, Y. Fu, L. Liu, Q.-X. Guo, Tetrahedron Lett. 49 (2008) 3458–3462.
[34] M. Shen, G. Li, B.Z. Lu, A. Hossain, F. Roschangar, V. Farina, C.H. Senanayake, Org. Lett. 6 (2004) 4129–4132.
[35] R.A. Komoroski, A.J. Magistro, P.P. Nicholas, Inorg. Chem. 25 (1986) 3917–3925.
[36] A.D. Zotto, C. Greco, W. Baratta, K. Siega, P. Rigo, Eur. J. Inorg. Chem. 18 (2007).
[37] M.R. Karasch, R.C. Seyler, F.R. Mayo, J. Am. Chem. Soc. 60 (1938) 882–884.
[38] M.A. Andrews, T.C.-T. Chang, C.-W.F. Cheng, T.J. Emge, K.P. Kelly, T.F. Koetzle, J. Am. Chem. Soc. 106 (1984) 5913–5920.